Glycobiology vol. 22 no. 10 pp. 1289–1301, 2012
doi:10.1093/glycob/cws103
Advance Access publication on June 26, 2012

Biosynthesis of the major brain gangliosides GD1a and GT1b

Elizabeth R Sturgill[2,†], Kazuhiro Aoki[3,†], Pablo HH Lopez[2], Daniel Colacurcio[2], Katarina Vajn[2], Ileana Lorenzini[2], Senka Majić[2], Won Ho Yang[4,5,6], Marija Heffer[7], Michael Tiemeyer[3], Jamey D Marth[4,5,6], and Ronald L Schnaar[1,2,8]

[2]Department of Pharmacology and Molecular Sciences, Johns Hopkins University School of Medicine, 725 N. Wolfe Street, Baltimore, MD 21205, USA; [3]Complex Carbohydrate Research Center, University of Georgia, Athens, GA 30602, USA; [4]Center for Nanomedicine, Sanford-Burnham Medical Research Institute and University of California Santa Barbara, Santa Barbara, CA 93106, USA; [5]Department of Molecular, Cellular, and Developmental Biology, and [6]Biomedical Sciences and Engineering Program, University of California Santa Barbara, Santa Barbara, CA 93106, USA; [7]Department of Medical Biology, J. J. Strossmayer University, School of Medicine, Osijek, Croatia; and [8]Department of Neuroscience, Johns Hopkins University School of Medicine, Baltimore, MD 21205, USA

Received on June 2, 2012; revised on June 19, 2012; accepted on June 22, 2012

Gangliosides—sialylated glycosphingolipids—are the major glycoconjugates of nerve cells. The same four structures—GM1, GD1a, GD1b and GT1b—comprise the great majority of gangliosides in mammalian brains. They share a common tetrasaccharide core (Galβ1–3GalNAcβ1-4Galβ1-4Glcβ1-1′Cer) with one or two sialic acids on the internal galactose and zero (GM1 and GD1b) or one (GD1a and GT1b) α2–3-linked sialic acid on the terminal galactose. Whereas the genes responsible for the sialylation of the internal galactose are known, those responsible for terminal sialylation have not been established in vivo. We report that *St3gal2* and *St3gal3* are responsible for nearly all the terminal sialylation of brain gangliosides in the mouse. When brain ganglioside expression was analyzed in adult *St3gal1*-, *St3gal2*-, *St3gal3*- and *St3gal4*-null mice, only *St3gal2*-null mice differed significantly from wild type, expressing half the normal amount of GD1a and GT1b. *St3gal1*/*2*-double-null mice were no different than *St3gal2*-single-null mice; however, *St3gal2*/*3*-double-null mice were >95% depleted in gangliosides GD1a and GT1b. Total ganglioside expression (lipid-bound sialic acid) in the brains of *St3gal2/3*-double-null mice was equivalent to that in wild-type mice, whereas total protein sialylation was reduced by half. *St3gal2/3*-double-null mice were small, weak and short lived. They were half the weight of wild-type mice at weaning and displayed early hindlimb dysreflexia. We conclude that the *St3gal2* and *St3gal3* gene products (ST3Gal-II and ST3Gal-III sialyltransferases) are largely responsible for ganglioside terminal α2-3 sialylation in the brain, synthesizing the major brain gangliosides GD1a and GT1b.

Keywords: brain / ganglioside / myelin / sialic acid / sialyltransferase

Introduction

The glycome of the mammalian brain is unusual in its relative abundance of glycolipids, which constitute >80% of brain glycans (Schnaar 2005). Among these, the major glycans of nerve cells are gangliosides, sialylated glycosphingolipids that carry most of the sialic acid in the brain (Kolter et al. 2002; Schnaar 2007; Yu et al. 2007; Todeschini and Hakomori 2008). Although there are hundreds of ganglioside structures based on sugar moieties alone (Yu et al. 2007), and many more when variation in the ceramide lipid carrier is considered, among mammals (and birds), four glycan structures predominate in the brain—GM1, GD1a, GD1b and GT1b—comprising up to 97% of gangliosides in the human brain (Svennerholm 1964; Tettamanti et al. 1973; Ando 1983). These four gangliosides (Figure 1) share the same neutral tetrasaccharide core (Galβ1-3GalNAcβ1-4Galβ1-4Glcβ1-1′Cer), with one or two sialic acids on the internal galactose (to make GM1 and GD1b, respectively) and an additional sialic acid on the non-reducing terminal galactose to make GD1a (from GM1) and GT1b (from GD1b). Gangliosides function in *cis*, modulating the activity of signaling proteins in their own membranes, and in *trans*, acting as receptors for complementary binding proteins on apposing cells (Todeschini and Hakomori 2008). As an example of the latter, gangliosides GD1a and GT1b on axons are functional ligands for the lectin myelin-associated glycoprotein (MAG, Siglec-4; Schnaar and Lopez 2009). Based on genetic, biochemical and cell biological studies, MAG on myelin binds to GD1a and GT1b on axons to help ensure long-term axon-myelin stability, protect axons from toxic insults and modulate axon regeneration. MAG binding to GD1a and GT1b is dependent on the terminal α2-3-linked sialic acid; it does not bind to GM1 or GD1b (Yang et al. 1996; Collins, Yang, et al. 1997). This and other

[1]To whom correspondence should be addressed: Tel: +1-410-955-8392; Fax: +1-410-955-3023; e-mail: schnaar@jhu.edu
[†]These authors contributed equally to this work.

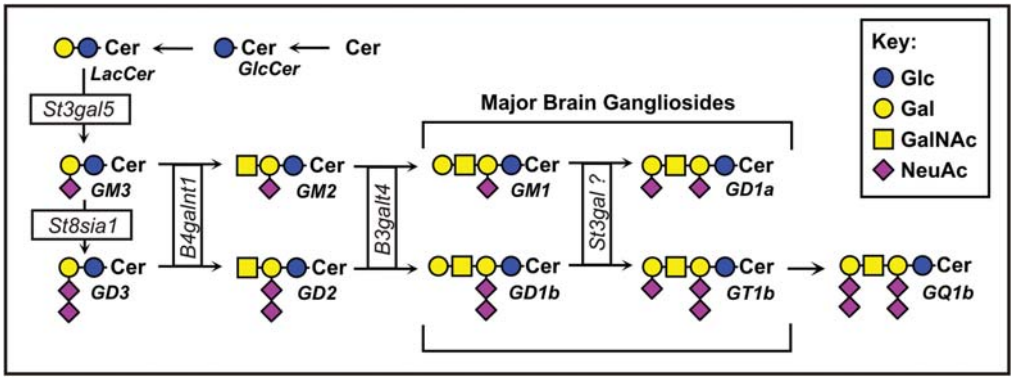

Fig. 1. Structures and biosynthetic pathways of the major brain gangliosides.

ganglioside structure–function relationships have been investigated in vivo using a series of mice with altered ganglioside biosynthetic enzyme genes (Proia 2003; Pan et al. 2005; Schnaar 2005).

Gangliosides (and other glycosphingolipids) are synthesized stepwise from ceramide by a sequential addition of sugars by a series of glycosyltransferases (Figure 1), most of which are specific for glycolipid biosynthesis, but others of which are involved in glycosylation of both glycolipids and glycoproteins (Kolter et al. 2002). The precursor to most gangliosides, lactosylceramide, is acted upon by the *St3gal5* gene product (ST3Gal-V) to make GM3, which may be acted upon further by the *St8sia1* gene product to make the disialoganglioside GD3. These become the "internal" sialic acids on the major brain gangliosides. Each of these is an acceptor for the same lipid-specific *N*–acetylgalactosaminyltransferase, the *B4galnt1* gene product, making GM2 (from GM3) and GD2 (from GD3), respectively. Once the GalNAc is added, further addition or removal of sialic acids on the internal galactose does not occur, and the pathway is fixed as the "a–series" (one internal sialic acid) or the "b-series" (two internal sialic acids). Although other gangliosides are found in the brain, such as the "0–series" (no internal sialic acids) and the "c–series" (three internal sialic acids), these are quantitatively minor.

Mice with a disrupted *St3gal5* gene fail to synthesize GM3 or any of the a-series or b-series gangliosides (Yamashita et al. 2003). Mice with a disrupted *St8sia1* gene do not make GD3 or the b–series gangliosides (Kawai et al. 2001). Identifying the enzyme(s) responsible for adding the terminal α2-3 sialic acid to GM1 and GD1b (GD1a and GT1b synthase(s), respectively) was the goal of the current study.

The mouse and human genomes encode six α2-3 sialyltransferases (ST3Gal-I through ST3Gal–VI, Table I; Audry et al. 2011). Using in vitro enzyme assays, ST3Gal-I and ST3Gal-II robustly add sialic acid to the terminal galactose of Galβ1-3GalNAc-terminated glycolipids (Kono et al. 1997) and were thought to synthesize GD1a and GT1b in vivo (http://www.kegg.jp/kegg/pathway.html and http://www.functionalglycomics.org), although this had not been confirmed genetically. ST3Gal–V and ST3Gal-VI fail to transfer sialic acid to GM1 and GD1b in vitro (Kono et al. 1998; Okajima et al. 1999) and are unlikely to be involved in GD1a or GT1b synthesis, although they cannot be definitively excluded. To establish the enzymes responsible for the biosynthesis of GD1a and GT1b, the current study evaluated the contributions of four mouse genes, *St3gal1* through *St3gal4* (Priatel et al. 2000; Ellies, Ditto, et al. 2002; Ellies, Sperandio, et al. 2002), individually and in combination.

Table I. ST3Gal sialyltransferases in mammals[a]

Gene	Enzyme	Gene synonyms	Ganglioside synthesis[b]	Brain expression[c]
St3gal1	ST3Gal-I	*Siat4, Siat4a*	+++	+/–
St3gal2	ST3Gal-II	*Siat4b, Siat5*	+++	++
St3gal3	ST3Gal-III	*Siat3, Siat6*	+	+++
St3gal4	ST3Gal-IV	*Siat4c*	+/–	+
St3gal5	ST3Gal-V	*GM3S, Siat9*	–	+++
St3gal6	ST3Gal-VI	*Siat10*	–	+

[a]Based on references Kono et al. (1997, 1998) and Okajima et al. (1999).
[b]Glycosphingolipid acceptor activity in vitro.
[c]Brain mRNA expression.

Results

Ganglioside expression in St3gal mutant mice

Gangliosides were extracted from the brains of young adult (6–12-week-old) *St3gal1*-, *St3gal2*-, *St3gal3*– and *St3gal4*-null mice and from wild-type littermates of each and analyzed by thin-layer chromatography (TLC). Wild-type mouse brain gangliosides had high levels of GD1a and GT1b, as well as GM1, GD3, GD1b, GQ1b and GT1b-OAc (GT1b bearing sialic acid(s) with a 9-*O*–acetyl group). Brain ganglioside patterns of *St3gal1*-, *St3gal3*- and *St3gal4*-null mice were indistinguishable from wild type. In contrast, *St3gal2*-null mouse brain gangliosides were diminished in GD1a and GT1b with a concomitant increase in GM1 and GD1b (Figure 2), a pattern consistent with partial loss of ganglioside terminal α2–3 sialylation (Figure 1). Quantitative densitometry revealed that gangliosides bearing an α2-3 NeuAc on the terminal galactose, together, comprise >60% of wild-type mouse brain gangliosides, a value reduced by half in *St3gal2*-null mice (Figure 3). Based on these data, ST3Gal-II is responsible for the biosynthesis of a significant proportion

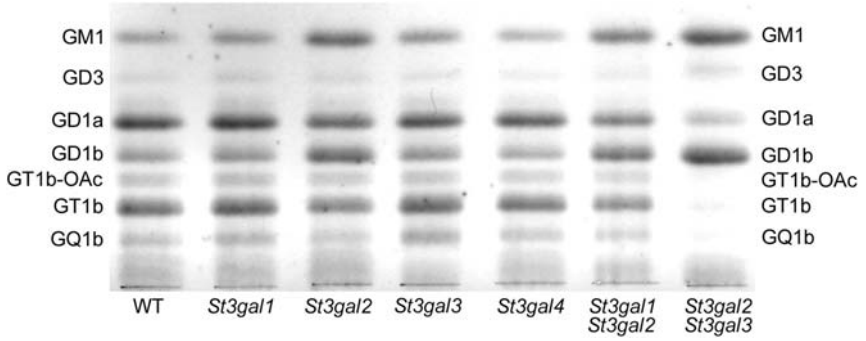

Fig. 2. TLC of mouse brain gangliosides from wild-type (WT) and *St3gal*-single- and *St3gal*-double-null mice.

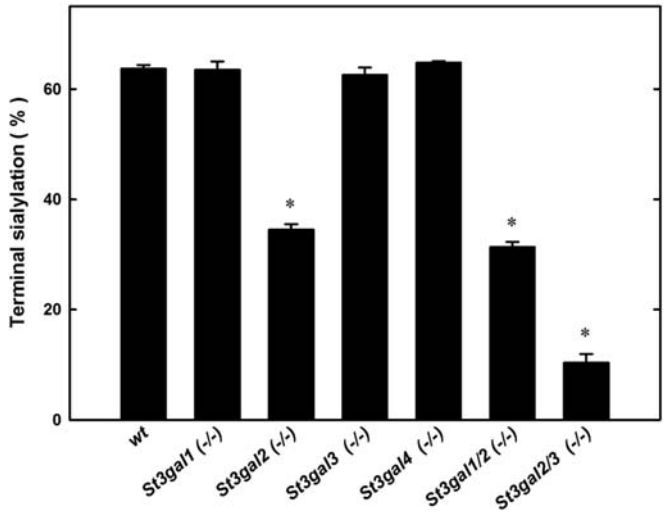

Fig. 3. Quantification of ganglioside terminal sialylation based on TLC densitometry. Gangliosides of wild-type (*wt*) and *St3gal* mutant mice were resolved by TLC, stained with resorcinol, scanned and the bands quantified by densitometry. Since resorcinol staining intensity is proportional to sialic acid content, each ganglioside band density was divided by the number of sialic acids on that ganglioside species. The sum of gangliosides with a NeuAc bound α2-3 to the terminal galactose (GD1a + GT1b + GT1b-OAc + GQ1b) was divided by the total of all ganglioside species to give the percent terminal sialylation. Values are the mean ± SEM for 2–14 individual mice of that genotype. $*P << 0.001$ compared with wild type.

of GD1a and GT1b, whereas one or more other sialyltransferases contribute to their biosynthesis and/or compensate in its absence.

Based on its published in vitro acceptor specificity (Table I), we tested whether ST3Gal-I was the major compensating enzyme. *St3gal1/2*-double-null mice, however, displayed a brain ganglioside pattern similar to that of *St3gal2*-single-null mice (Figures 2 and 3), suggesting that ST3Gal-I is not a major compensating enzyme. Based on its relatively high expression level in the brain (Table I), we next tested whether ST3Gal-III was involved in ganglioside biosynthesis by breeding *St3gal2/3*-double-null mice. Notably, the brain gangliosides from these mice lacked GT1b and GQ1b, had diminished GD1a and instead expressed increased amounts of GM1 and GD1b. Based on these data, we conclude that ST3Gal-III contributes to GD1a and GT1b biosynthesis in vivo and is primarily responsible for ganglioside terminal α2–3 sialylation in the absence of ST3Gal-II. By TLC, it appeared that while GT1b was nearly absent in *St3gal2/3*-double-null mice, a considerable amount of GD1a remained (Figure 2). However, mass spectrometry (MS) and two-dimensional TLC modified this conclusion.

MS was performed on permethylated and native (unpermethylated) brain gangliosides from wild-type and *St3gal2/3*-double-null mice. Linear trap quadrupole (LTQ) MS of permethylated brain gangliosides indicated nearly complete disappearance of GT1 and GQ1 species in the *St3gal2/3*-double-null brain, with GM1 and GD1 masses predominating (Figure 4A). MS^n analyses distinguished isomeric gangliosides, revealing that GD1 was predominantly GD1a in wild-type mice, but was nearly all GD1b in *St3gal2/3*-double-null mice (Figure 4B, Supplementary data, Figure S1). These MS data strongly support the conclusion that ST3Gal-II and -III are responsible for GD1a and GT1b biosynthesis. Combined disruption of *St3gal2* and *St3gal3* genes resulted in a reduction in both GD1a and GT1b to <5% of their corresponding wild-type levels (Figure 5).

Compared with MS detection, one-dimensional TLC analysis (Figures 2 and 3) overestimated the abundance of GD1a. Since sialic acids on brain gangliosides may be *O*–acetylated, and *O*–acetylated gangliosides migrate more rapidly on TLC, the MS data raised the possibility that the species co-migrating with GD1a in *St3gal2/3*-double-null mouse brain gangliosides was an *O*–acetylated form of GD1b (GD1b-OAc). *O*–Acetylated structures would have been missed in the MS analysis of permethylated gangliosides, since permethylation is performed under alkaline conditions that cleave these esters. Therefore, we used two-dimensional TLC and MS of native gangliosides to resolve this question.

Two-dimensional TLC was performed in which intact gangliosides were resolved in one dimension, the plate was treated with alkali (ammonia vapor) to hydrolyze *O*–acetyl groups (and other alkali-sensitive groups) and then the plate was developed with the same solvent in the orthogonal direction. Alkali-stable gangliosides migrate equally in both dimensions, resulting in a diagonal array (Figure 6). Alkali-sensitive gangliosides migrate slower in the second dimension, appearing below the diagonal. Their migration in the second dimension defines the parent ganglioside. In wild-

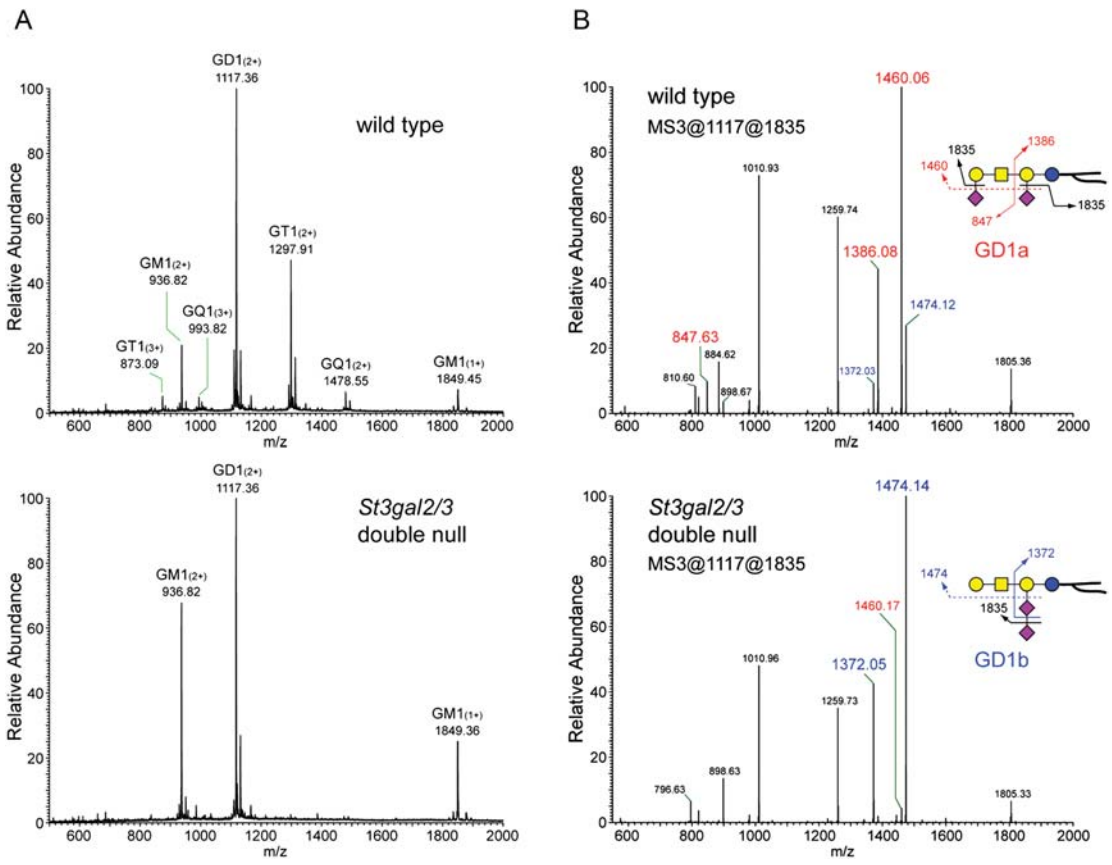

Fig. 4. MS of permethylated wild-type and *St3gal2/3*-double-null mouse brain gangliosides. (**A**) Region of the full MS showing major brain gangliosides, with GT1 and GQ1 species diminished in *St3gal2/3*-double-null mouse brain gangliosides. (**B**) MS3 analyses of the permethylated disialoganglioside peaks of wild-type and mutant mouse brains demonstrating the relative intensity of GD1a-related fragments (red labels) and GD1b-related fragments (blue labels).

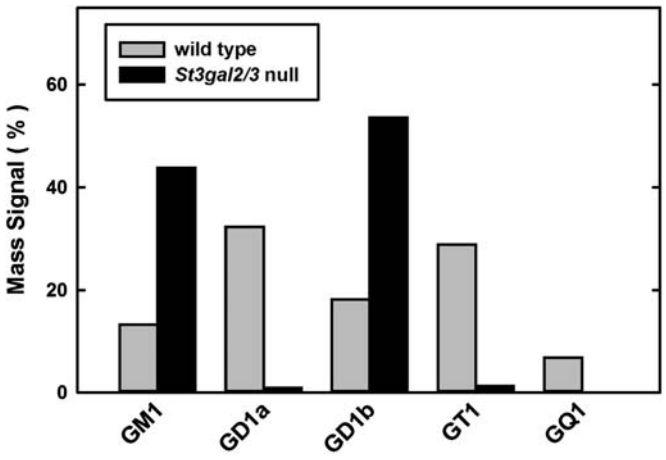

Fig. 5. Quantification of MS peak intensities of permethylated gangliosides from wild-type and *St3gal2/3*-double-null mice.

type mice, GD1a and other major brain gangliosides are prominent on the diagonal, and alkali-sensitive forms of GD1b, GT1b and GQ1b also appear. In *St3gal2/3*-double-null mouse brain gangliosides, GD1a is nearly absent on the diagonal, but there is a prominent alkali-sensitive form of GD1b that co-migrates with GD1a in the first dimension, explaining the apparent discrepancy between one-dimensional TLC and MS quantifications of permethylated brain gangliosides in these mutants. Notably, *O*–acetylated forms of GD1b are minor components of wild-type mouse brain gangliosides, where *O*–acetylated forms of GT1b and GQ1b are more common. In *St3gal2/3*-double-null mice, the *O*–acetylation of GD1b is markedly increased.

MS analysis of intact gangliosides confirmed the presence of *O*–acetylated gangliosides initially demonstrated by two-dimensional TLC. Whereas non-acetylated forms of GD1 are quantitatively equivalent in wild-type and *St3gal2/3*-double-null brain gangliosides, GD1-OAc (GD1b-OAc based on 2D TLC) is increased in the mutant (Figure 7). Total ion mapping (TIM) MS data were acquired and the resulting MS2 profiles were filtered for the presence of a signature fragment ion that indicates *O*–acetylated sialic acid ($m/z = 332.2$). TIM profiles demonstrated that GD1 was the exclusive carrier of *O*–acetyl groups in brain gangliosides from mutant mice. Quantification of *O*–acetylated species by TIM MS of intact gangliosides confirmed the shift from GT1 to GD1 *O*–acetylation in the mutant mice, along with increased GD1b lactone (Figure 8).

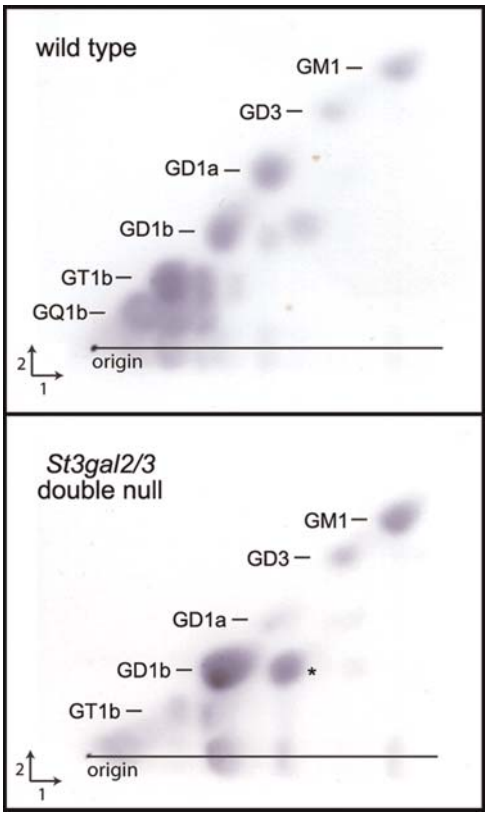

Fig. 6. Two-dimensional TLC of brain gangliosides from wild-type and *St3gal2/3*-double-null mice. An aliquot (2 μL) of purified brain ganglioside mixture from each mouse was applied at the origin and resolved in the first dimension in chloroform/methanol/0.25% aqueous KCl (60:35:8). The plate was dried, exposed to ammonia vapor overnight, dried and resolved in the second dimension using the same solvent. Spots were detected using a resorcinol reagent (Schnaar and Needham 1994). Spots falling below the diagonal are alkali sensitive. The major alkali-sensitive spot in the mutant ganglioside extract (*) was independently identified as GD1b-OAc.

We conclude from the above analyses that ST3Gal-II and ST3Gal-III are responsible for the great majority of ganglioside terminal α2-3 sialylation in the brain. Further MS data consistent with this conclusion are as follows. (i) Terminally sialylated monosialoganglioside (GM1b) is a minor component of wild-type mouse brain, but is absent from *St3gal2/3*-double-null mice (Supplementary data, Figure S2). (ii) GT1c, which is triply sialylated on the internal galactose, is absent from wild-type mice but present as a minor component in *St3gal2/3*-double-null mice (Supplementary data, Figure S3).

Glycolipid and glycoprotein sialylation in St3gal mutant mice

St3gal2-null and *St3gal2/3*-double-null mice had the same total level of lipid-bound sialic acid in their brains, despite changes in the species of gangliosides expressed (Figure 9). *St3gal1*-, *St3gal2*- and *St3gal4*-single-null mice displayed no decrease in total brain protein or lipid sialylation. While *St3gal3*-null mice had no change in lipid-bound sialic acid, a 36% decrease in glycoprotein-bound sialic acid was observed when compared with wild-type mice ($P < 0.001$). In *St3gal2/3*-double-null mice, glycoprotein sialylation was reduced even further, to less than half compared with wild-type mice ($P < 0.001$ vs wild type, $P < 0.05$ vs *St3gal3* single null).

Ganglioside immunohistochemistry in St3gal mutant mice

High-specificity anti-ganglioside antibodies were used to probe the presence and distribution of major brain gangliosides in sagittal sections of wild-type and *St3gal2/3*-double-null mice (Figure 10). In wild-type mice, GM1 immunostaining was abundant in white matter but diminished in grey matter. In contrast, GM1 immunostaining was robustly increased in grey matter of double-null mice. GD1b immunostaining was apparent throughout the brains of both wild-type and double-null mice. GT1b immunostaining was detected throughout the brain of wild-type mice, with higher density in grey matter than white matter. In the double-null mice, GT1b immunostaining was reduced to background levels. Interestingly, GD1a immunostaining, which is primarily in the grey matter in the brains of wild-type mice, was greatly reduced but not absent in the double-null mouse brain. The GD1a immunostaining that remained in *St3gal2/3*-double-null mice appeared in a rostral to caudal gradient, with GD1a immunostaining absent from the cerebellum (for example) and present in the olfactory bulb and far rostral forebrain.

In contrast to the changes seen in *St3gal2/3*-double-null mice, immunohistochemical ganglioside patterns in *St3gal3*-single-null mice were grossly indistinguishable from wild type (Supplementary data, Figure S4). In *St3gal2*-single-null mice, GM1 immunostaining was expanded, GD1a staining was selectively diminished, notably in caudal brain areas, and the histological distribution of GD1b and GT1b was not different from wild type.

Prior studies indicated that GD1a and GT1b bind specifically to MAG and that the absence of complex gangliosides including GD1a and GT1b in *B4galnt1*-null mice resulted in progressive axon-myelin instability and progressively diminished steady-state levels of MAG in the brains of older mutant mice (Sun et al. 2004). In St3gal2/3-double-null mice, MAG immunostaining was greatly diminished compared with wild-type mice, even at 4–6-weeks old (Figure 11). In comparison with *St3gal2/3*-double-null mice, MAG immunostaining in *St3gal3*-single-null mice was not diminished and that in *St3gal2*-single-null mice was slightly reduced (Supplementary data, Figure S5). These data are consistent with steady-state MAG expression being related to the presence of MAG-binding brain gangliosides.

Phenotypes of St3gal mutant mice

Whereas *St3gal2*-single-null mice appeared robust, *St3gal3*-single-null mice were not as robust as wild-type mice, were smaller at weaning and were relatively poor breeders. Crosses of *St3gal3*-heterozygous mice resulted in somewhat fewer *St3gal3*-single-null offspring than predicted (Table II, $P = 0.03$, χ^2 test). Compared with the *St3gal3*-single-null mice, the *St3gal2/3*-double-null mice were yet smaller, weaker, short-lived (few lived past 8 weeks) and did not breed when they reached maturity. Crosses of mice that were null at the *St3gal2* gene locus and heterozygous for the *St3gal3* gene

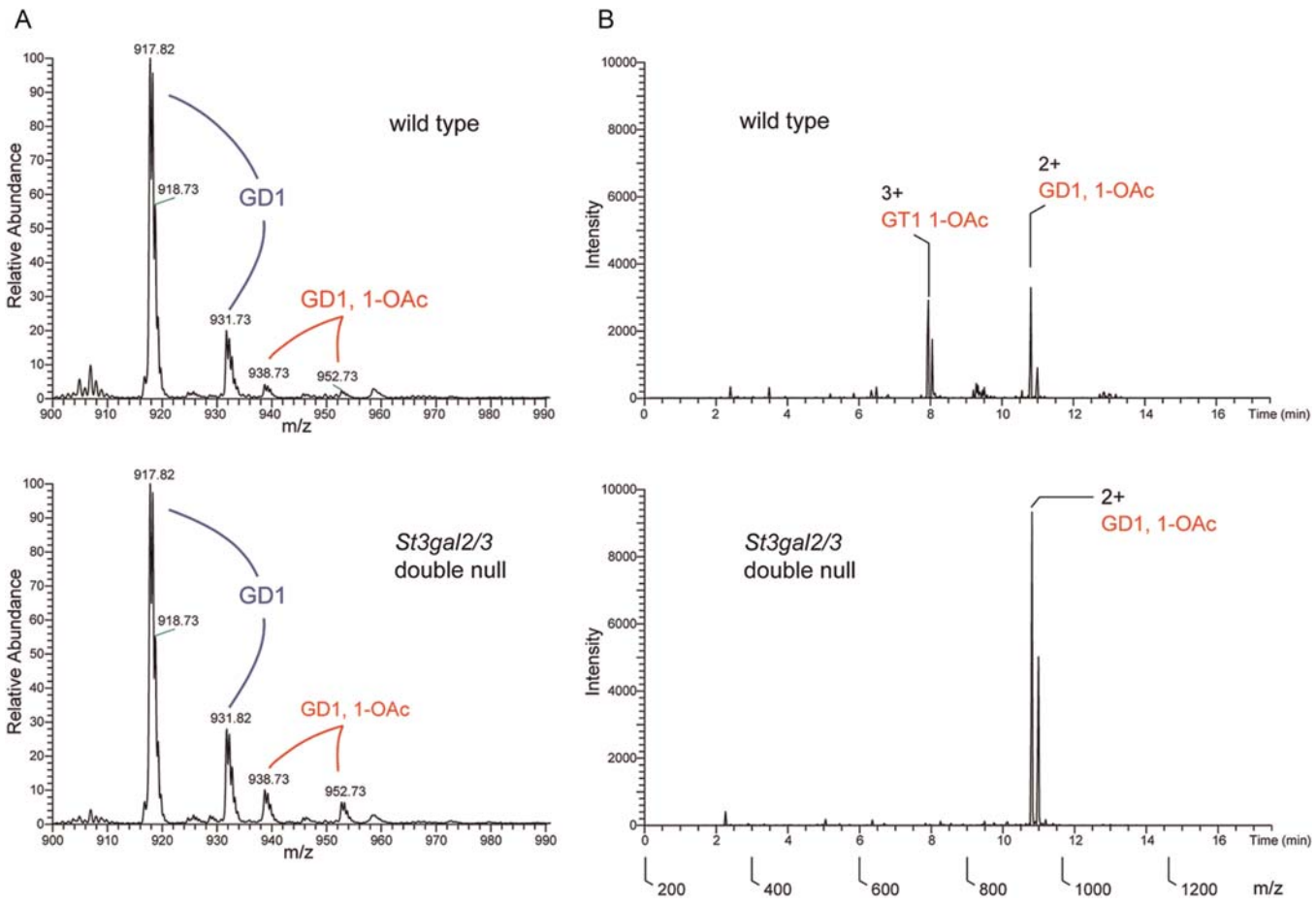

Fig. 7. MS of native gangliosides from wild-type and *St3gal2/3*-double-null mice. (**A**) Full MS of the *m/z* range containing GD1 (GD1a and GD1b) and monoacetylated forms of GD1in the wild-type and mutant brain gangliosides. Note the higher abundance of GD1-OAc in the mutant mice. (**B**) Total ion maps filtered for the presence of the fragment ion 332.2, the signature loss of an *O*–acetylated sialic acid. Note the absence of GT1-OAc and the increase in GD1-OAc in the mutant, resulting in the maintenance of total *O*–acetylated ganglioside sialic acid in the mutant. The double peaks for each ganglioside result from different ceramide (sphingosine) lengths.

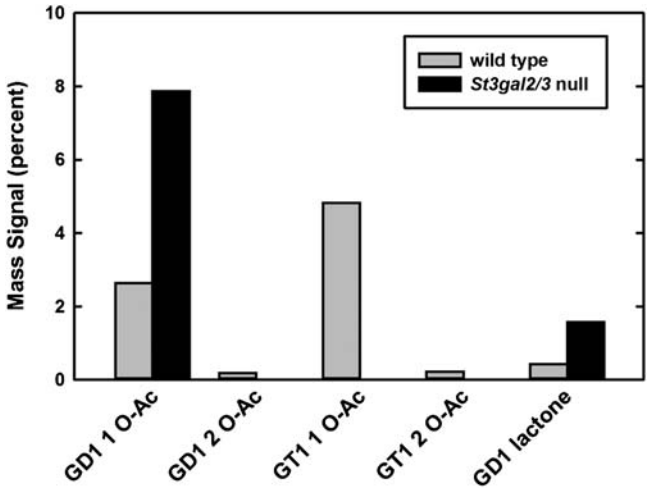

Fig. 8. Quantification of MS peak intensities of native *O*–acetylated and lactone forms of gangliosides from wild-type and *St3gal2/3*-double-null mice. Note the quantitative shift of *O*–acetylation from GT1 to GD1 (presumably GD1b) species in the mutant.

resulted in markedly fewer double-null offspring than predicted (Table II, $P < 10^{-9}$, χ^2 test). *St3gal2/3*-double-null mice that did survive were half the size of their wild-type counterparts (Figure 12).

In a preliminary test of nervous system function, the hindlimb reflex was determined at weaning. When wild-type mice are lifted gently by the tail, they typically spread their hindlimbs to >90° angle (Figure 13A). In contrast, double-null mice usually fail to spread their hindlimbs, instead clasping them close to their body (Figure 13B). Quantification of the hindlimb reflex response revealed that *St3gal2*-null mice were normal, *St3gal3*-null mice were partially impaired and *St3gal2/3*-double-null mice were severely impaired at weaning (Figure 13C).

Discussion

Gangliosides, the most abundant sialoglycans in the brain, are prominent structural determinants on all mammalian nerve cells and axons (Schnaar 2007; Maccioni et al. 2011).

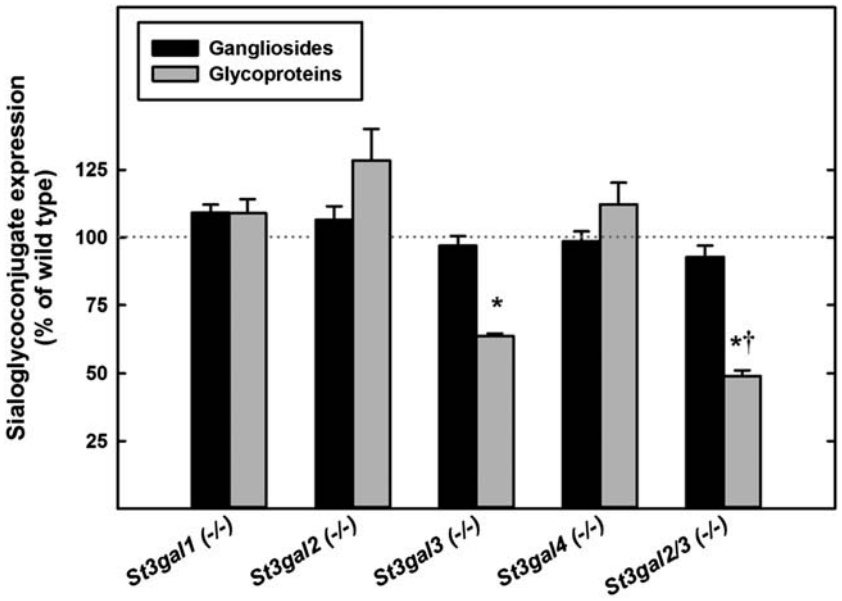

Fig. 9. Changes in glycolipid and glycoprotein sialylation relative to wild-type mice in *St3gal* mutants. Total glycolipid sialylation was determined from TLC scans and total glycoprotein sialylation from Dionex sialic acid quantification after the hydrolysis of de-lipidated brain proteins as described in the text. For each mouse mutant, the change in glycolipid (ganglioside) and glycoprotein sialylation with respect to the wild-type brain is shown. Values are the mean ± SEM for 2–8 individual mice of that genotype. *$P < 0.001$ vs wild type; †$P < 0.05$ vs *St3gal3*-null.

In mammals (and birds), the same four ganglioside structures predominate (Tettamanti et al. 1973; Svennerholm et al. 1989): GM1, GD1a, GD1b and GT1b (Figure 1). Depending on the exact site in the human brain (Kracun et al. 1984), about half of ganglioside sialic acid is carried on two structures, GD1a and GT1b, which are synthesized from GM1 and GD1b (respectively) by addition of an α2-3-linked sialic acid on the non-reducing terminal galactose of the gangliotetraose core, forming an NeuAcα2-3Galβ1-3GalNAc arm. Among the potential functions of gangliosides in the brain, GD1a and GT1b have been implicated in the maintenance and regulation of myelin-axon interactions based on their binding to MAG, a sialic acid-binding lectin of the Siglec family (Siglec-4; Schnaar 2010). Detailed analysis of MAG-glycan binding revealed that the terminal α2-3 sialic acid on the NeuAcα2-3Galβ1-3GalNAc arm is essential for recognition (Yang et al. 1996; Collins, Kiso, et al. 1997). Further exploration of the role of GD1a and GT1b functions would benefit from a mouse genetic model in which GD1a and GT1b terminal sialylation were abrogated.

Our findings reported here establish that, in the mouse, ST3Gal-II is primarily responsible for ganglioside terminal sialylation, with ST3Gal-III also capable of synthesizing significant amounts of GD1a and GT1b in vivo. We base these conclusions on the observation that *St3gal2*-null mice are significantly depleted in GD1a and GT1b, whereas *St3gal1*-, *St3gal3*- and *St3gal4*–null have normal ganglioside profiles. However, *St3gal2/3*-double-null mice have profoundly diminished GD1a and GT1b expression. Surprisingly our evidence does not support the involvement of ST3Gal-I in GD1a and GT1b biosynthesis in the brain. ST3Gal-I was thought to contribute to ganglioside biosynthesis based on its robust ability to terminally sialylate GM1 and gangliotetraosylceramide (asialo-GM1) in vitro (Lee et al. 1993; Kono et al. 1997), although its preference for *O*–linked glycoproteins had been predicted (Kojima et al. 1994). Consistent with the latter observation, *St3gal1* gene expression is relatively high in the salivary gland and spleen, but low in the adult mouse brain (Kono et al. 1997). While we cannot rule out a minor role for ST3Gal-I in the biosynthesis of GD1a and GT1b in the brain (or in other tissues), *St3gal1* gene disruption had no significant effect on brain ganglioside expression either alone or in combination with *St3gal2* gene disruption.

A consistent observation of several genetic studies that have disrupted ganglioside biosynthetic pathways has been the finding that total brain ganglioside levels are maintained despite changes in the individual ganglioside species expressed (Takamiya et al. 1996; Liu et al. 1999; Kawai et al. 2001; Proia 2003; Yamashita et al. 2003). For example, *B4galnt1*-null mice (Figure 1) express the simple gangliosides GM3 and GM2 at concentrations that maintain the total brain gangliosides at the same level found in the wild-type mouse brain (Sun et al. 2004). Likewise, *St8sia1*-null mice express increased GM1 and GD1a such that the total brain ganglioside expression remains at wild-type levels (Kawai et al. 2001). Likewise, blocking *St3gal2/3* did not change the total level of ganglioside sialic acid in the brain, despite the shift in the ganglioside pattern. Remarkably, mice with a disrupted *St3gal5* gene express high levels of the otherwise rare "0–series" gangliosides (GM1b and GD1α) such that the total brain ganglioside levels remain similar to those in wild-type mice (Yamashita et al. 2003). Together, these data imply competitive or feedback mechanisms that maintain a narrow range of total ganglioside expression in the brain.

An additional level of ganglioside structural diversity is sialic acid *O*–acetylation (Sonnino et al. 1983; Varki 1992;

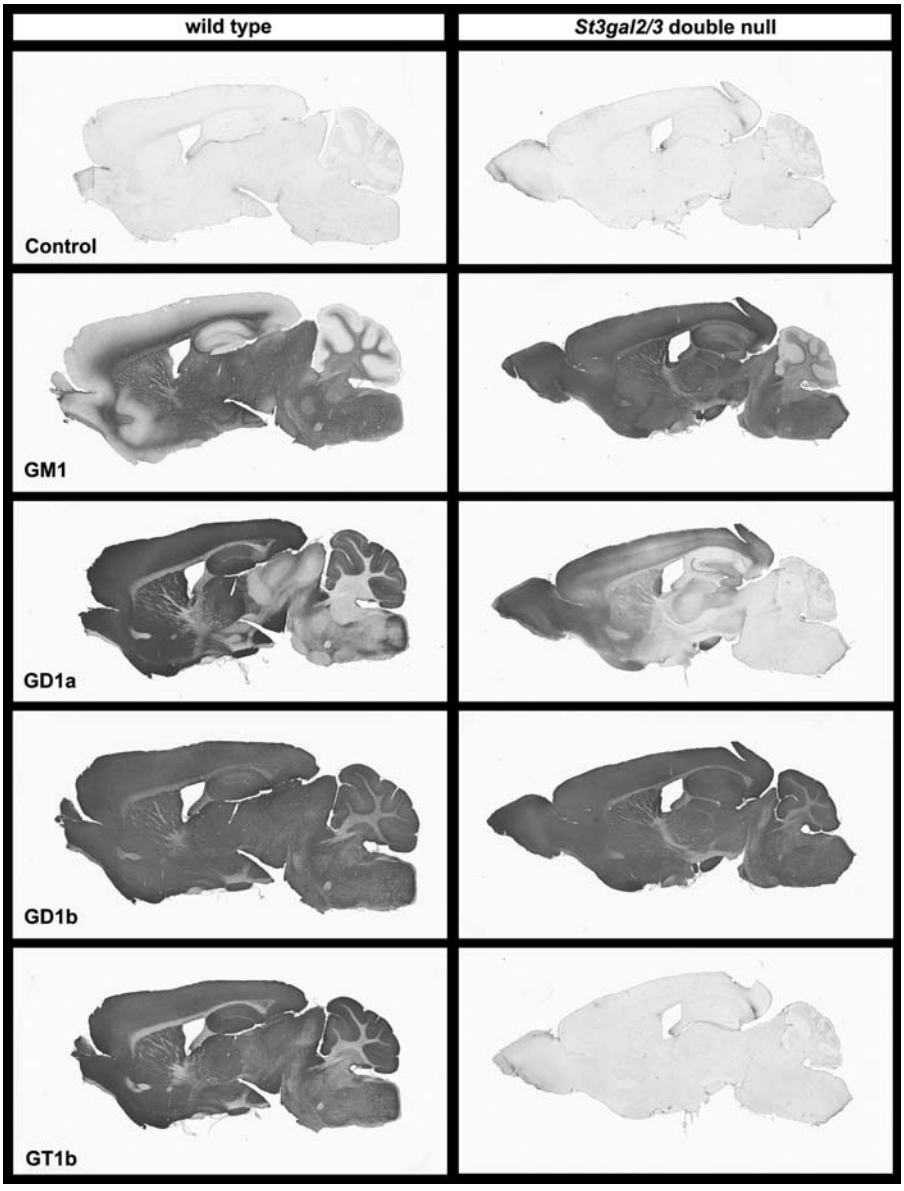

Fig. 10. Ganglioside immunohistochemistry on wild-type and *St3gal2/3*-double-null mouse mid-sagittal brain sections. Note the expansion of GM1 immunostaining from white matter only to throughout the brain in the mutant mice. Also note the absence of GT1b immunostaining and the greatly diminished GD1a immunostaining in the mutant mice, with the latter appearing in a rostral (left) to caudal (right) gradient.

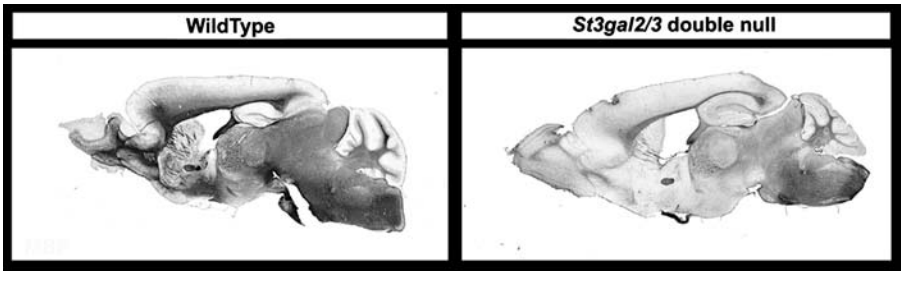

Fig. 11. MAG immunostaining in wild-type and *St3gal2/3*-double-null mice.

Table II. Offspring of *St3gal2*/*St3gal3* interbreedings[a]

St3gal3 genotype	St3gal2 wild-type St3gal3 heterozygote			St3gal2 null St3gal3 heterozygote		
	Genotype predicted	Genotype observed[b]	Percent observed	Genotype predicted	Genotype observed[c]	Percent observed
Wild type	31	41	33	64	93	36
Heterozygote	62	63	51	128	142	56
Null	31	20	16	64	21	8

[a]Breeding pairs of like genotype; offspring genotyped at weaning.
[b]χ^2 probability = 0.03.
[c]χ^2 probability = 3.5×10^{-10}.

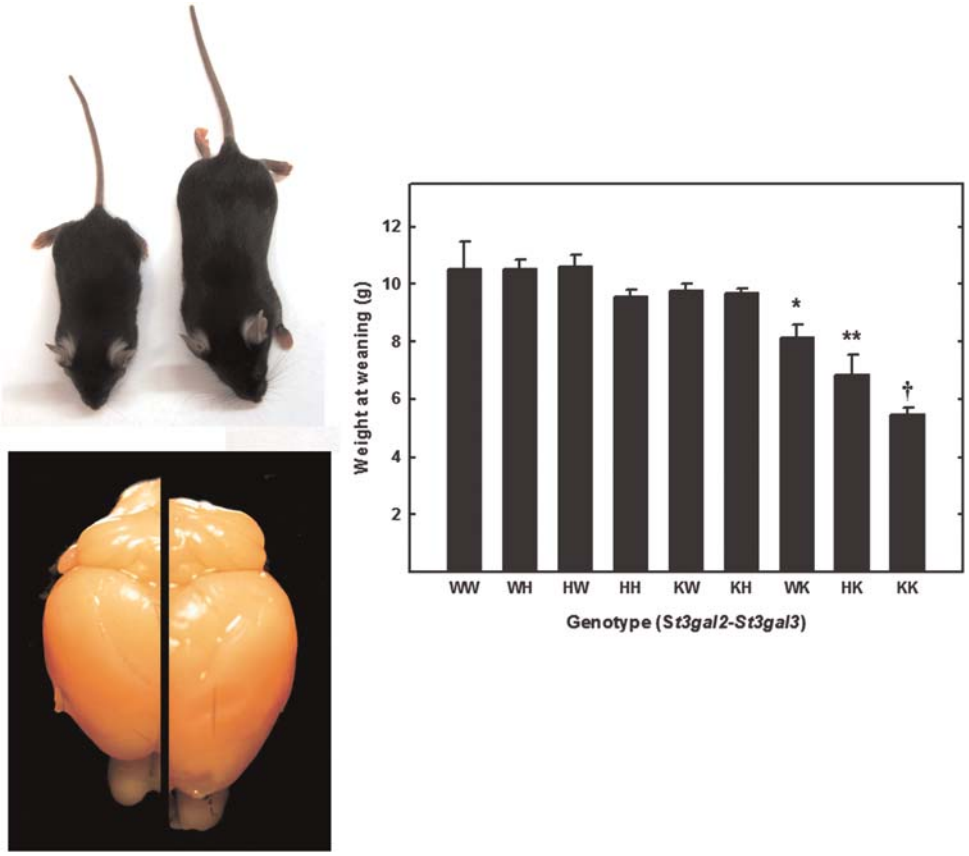

Fig. 12. Size of wild-type and *St3gal* mutant mice. Wild-type mice (right in photographs) are larger and have larger brains than mutant mice. Mice were weighed at weaning (21 days). The weights of wild-type mice (WW) and mice with mutations of their *St3gal2* and *St3gal3* genes are shown. The genotypes of the mice are designated as "XY", where "X" is the genotype of *St3gal2* and "Y" the genotype of *St3gal3*, with letter designations as "W", wild type; "H", heterozygote; "K", null. Values are the mean ± SEM for 6–81 individual mice. $*P < 0.05$; $**P < 0.01$; $^{\dagger}P << 0.001$.

Schauer 2009). Gangliosides with *O*–acetyl sialic acids comprise a few percent of total brain gangliosides in the mouse (Figures 6–8), mostly consisting of mono- and di-*O*–acetylated forms of GT1b, but also *O*–acetylated GQ1b and GD1b. In *St3gal2/3*-double-null mice, GT1b and GQ1b are essentially absent, but total ganglioside *O*–acetylation is similar to that in wild-type mice due to a complementary increase in *O*–acetylated GD1b. Again, there appear to be competitive or feedback mechanisms that maintain total ganglioside sialic acid *O*–acetylation at similar levels in wild-type and *St3gal2/3*-double-null mice. The functional role(s) of *O*–acetyl groups on brain gangliosides has yet to be determined.

In *St3gal2/3*-double-null mice, levels of GD1a and GT1b drop to near 1% of total gangliosides (Figure 5) but are not absent. This implies that other ST3Gal enzymes may also terminally sialylate gangliosides to a small extent. Based on in vitro acceptor specificities alone (Kono et al. 1997), ST3Gal–I may be responsible, but other ST3Gal enzymes cannot be excluded. The finding that the small amount of remaining GD1a in *St3gal2/3*-double-null mice appears in a rostral-caudal gradient may imply that the remaining ST3Gal enzyme

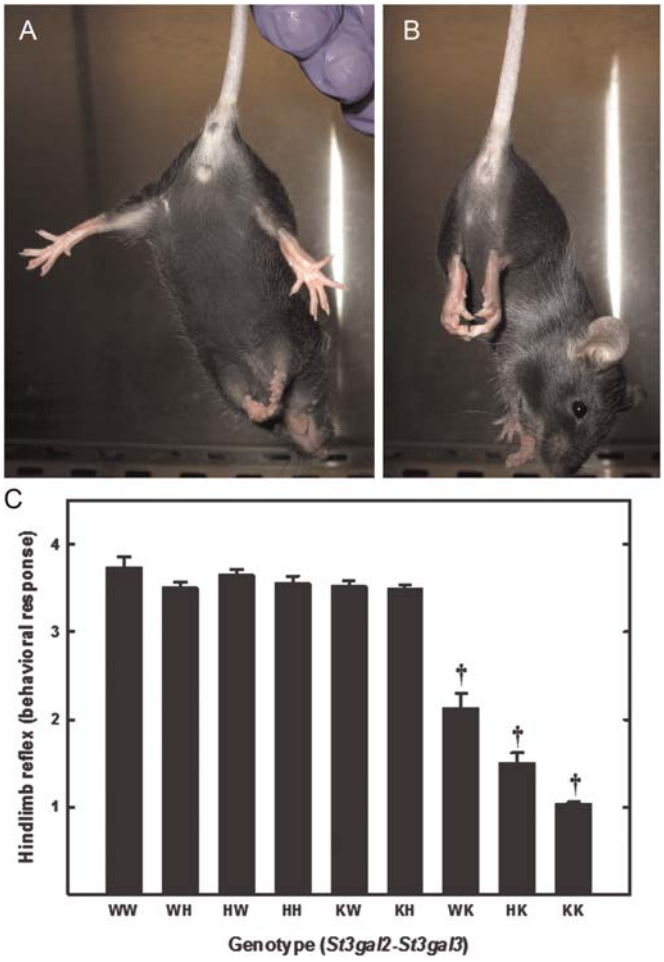

Fig. 13. Hindlimb reflex responses of wild-type and *St3gal* mutant mice. Wild-type mice (**A**) display a normal hindlimb response, extending their legs at a >90° angle, whereas *St3gal2/3*-double-null mice (**B**) display areflexia, with hindlimbs turned in and held close to the body. (**C**) Hindlimb reflex responses were quantified at weaning (21 days) as described in the text. Responses of wild-type mice (WW) and mice with mutations of their *St3gal2* and *St3gal3* genes are shown, with genotypes designated as described in the legend of Figure 12. Values are the mean ± SEM for 6–81 individual mice. $^{\dagger}P << 0.001$.

(s) responsible are expressed in a rostral-caudal gradient in the brain.

St3gal2/3-double-null mice are severely impaired. They do not produce offspring, and in heterozygote crossings the double-null mice survive (to weaning) at a rate significantly below normal. Those that survive are small, weak, short-lived (typically succumbing within 8 weeks) and display deficits in nerve function (the hindlimb reflex) at an early age. Some of these outcomes may be due to changes in ganglioside expression in the brain. However, relating phenotypic observations to changes in brain ganglioside sialylation per se, in this animal model, has not yet been studied, since the mice used here lack ST3Gal-II and ST3Gal–III in all tissues. The loss of these two sialyltransferases will impact glycolipid and glycoprotein sialylation inside and outside the brain, potentially contributing to the phenotype. For example, *St3gal3*-single-null mice display significant reductions in weight and hindlimb reflexes at weaning despite expressing normal brain ganglioside patterns. Even though these deficits are exacerbated in the *St3gal2/3*-double-null mice, ganglioside sialylation cannot be attributed for any of the phenotypes without additional experimental support. On the other hand, inappropriate or incomplete sialylation can be related, directly or indirectly, to causation of all of the phenotypes.

In conclusion, genetic experiments in the mouse establish ST3Gal-II and ST3Gal-III as the mammalian sialyltransferases primarily responsible for GD1a and GT1b biosynthesis in the brain in vivo. Their absence results in marked loss of GD1a and GT1b with comparable increases in their precursors, GM1 and GD1b. Although *St3gal2/3*-double-null mice have severe phenotypic deficits that may be related to ganglioside expression, the impact of changing glycoprotein and glycolipid sialylation throughout the animal from early embryonic development makes it difficult to link particular sialoglycan structures to specific functions without additional data. Nevertheless, qualitative and quantitative sialylation by these two of the six *St3gal* genes have proven profoundly important in development and viability.

Materials and methods

Mice

St3gal1-, *St3gal2*-, *St3gal3*- and *St3gal4*-null mice were produced by targeted gene disruption as described previously (Priatel et al. 2000; Ellies, Ditto, et al. 2002; Ellies, Sperandio, et al. 2002). Genotypes were determined using polymerase chain reaction (PCR) with primers 5′–CTTTG CGACAGGGTTTCATT and 5′–CAGGGTTGCTCAACAAG TG for disrupted *St3gal2* and 5′–GGGGATCTGAGGTCCT CTTCTGGAC and 5′–TAACCCCGAGGACTATGCTGGCT TG for disrupted *St3gal3*. Alternatively, genotyping was outsourced for determination by real-time PCR (Transnetyx, Cordova, TN). All procedures were approved by institutional Animal Care and Use Committees and were consistent with federal law and NIH regulations.

Ganglioside isolation and TLC analyses

Mice were decapitated, brains quickly dissected, bisected in the sagittal plane and snap frozen. For ganglioside extraction (Schnaar 1994), half brains were weighed, thawed on ice, added to 4 volumes of ice-cold water and homogenized 10 strokes in a Potter–Elvehjem glass-Teflon homogenizer on ice. Methanol was added to give a methanol/aqueous ratio of 8:3. The suspension was mixed vigorously and brought to ambient temperature, and then chloroform was added at half the volume of methanol to give a chloroform/methanol/aqueous ratio of 4:8:3. The suspension was further mixed, transferred to a glass centrifuge tube with a Teflon-lined cap, and the insoluble material removed by centrifugation (1200 × *g*, 15 min, ambient temperature). The supernatant was recovered, its volume measured and 0.173 volumes of water added, resulting in a two-phase solution. After vigorous mixing, the phases were separated by centrifugation as above, the upper (polar) phase collected and the lower phase discarded. The upper phase was evaporated at 45°C under a stream of

nitrogen; the residue dissolved in 2 mL of water and dialyzed for ≥24 h against water, using 1000-MW cut-off dialysis tubing (Spectrum Laboratories, Rancho Dominquez, CA). After dialysis, the aqueous solution was recovered, evaporated to dryness as above, and redissolved in chloroform/methanol/water (4:8:3) at a volume of 2 µL/mg of original brain tissue.

TLC was performed as described previously (Schnaar and Needham 1994) by spotting 1 µL of purified brain ganglioside (corresponding to 0.5 mg of original brain weight) and using chloroform/methanol/0.25% aqueous potassium chloride (60:35:8) as developing solvent. Resolved gangliosides were detected using a sialic acid-sensitive resorcinol spray reagent. Images of the developed, stained plates were scanned and analyzed for relative ganglioside intensities using Scion Image (Scion Corp., Frederick, MD).

Two-dimensional TLC (Sonnino et al. 1983) was performed by spotting 2 µL of purified brain ganglioside (corresponding to 1 mg of original brain weight), resolving in the first dimension as above, drying the plate and exposing it overnight to ammonia vapors in a closed chamber to hydrolyze alkali-labile groups. After thorough evaporation of residual ammonia, the plate was developed in the orthogonal dimension and gangliosides detected using the resorcinol reagent.

Ganglioside MS

Nanospray ionization MS was performed on native and permethylated gangliosides. For MS of native gangliosides, ~2.5 nmol of native total ganglioside were reconstituted in 50 µL of methanol/2–propanol/1-propanol/13 mM aqueous ammonium acetate (16:3:3:2 by volume) for infusion. For MS of permethylated gangliosides, ~0.5 nmol of permethylated total gangliosides were dissolved in 50 µL of 1 mM sodium acetate in methanol/water (1:1) for infusion. Both preparations were analyzed by infusion into a linear ion trap mass spectrometer (LTQ; Thermo Fisher Scientific, Waltham, MA) using a nanoelectrospray source at a syringe flow rate of 0.40 µL/min and capillary temperature set to 210°C (Anumula and Taylor 1992; Vukelic et al. 2005; Aoki et al. 2007; Nimrichter et al. 2008). Native gangliosides were analyzed in the negative mode and permethylated gangliosides were analyzed in the positive mode. The instrument was tuned with a mixture of permethylated standard neutral glycosphingolipids for the positive-ion mode and with native (unpermethylated) ganglioside GM1 for the negative-ion mode. For fragmentation by collision-induced dissociation (CID) in tandem mass spectrometry (MS/MS) and MS^n, a normalized collision energy of 30–35% was used.

Detection and relative quantification of the prevalence of individual gangliosides was accomplished using the TIM and neutral loss scan (NL scan) functionalities of the Xcalibur software package version 2.0 (Thermo Fisher Scientific) as described previously (Aoki et al. 2007). Briefly, for TIM, the *m*/*z* range from 500 to 2000 was automatically scanned in successive 2.8 mass unit windows with a window-to-window overlap of 0.8 mass units, which allowed the naturally occurring isotopes of each glycolipid species to be summed into a single response, thereby increasing detection sensitivity. Most ganglioside components were identified as singly, doubly, and triply charged, sodiated species (M + Na) in the positive mode. Peaks for all charge states were summed for quantification. For NL scans, an MS workflow was defined in which the highest intensity peak detected by full MS was subjected to CID fragmentation. Preliminary analysis demonstrated that the major fragment ions in CID MS/MS scans of glycolipid preparations correspond to the NL of the ceramide moiety, leaving intact glycolipid oligosaccharide ions. Therefore, the NL scan workflow was set to acquire MS^n fragmentation if an MS/MS profile contained an ion with *m*/*z* equivalent to loss of the most prevalent ceramide moiety. Following this data-dependent acquisition, the workflow returned to the full MS, excluded the parent ion just fragmented, and chose the peak of next highest intensity for the same MS/MS and MS^n analyses. By this data-dependent acquisition workflow, glycolipid glycan profiles and MS^n sequencing were rapidly acquired for complex mixtures of brain gangliosides. Glycolipid standards for MS analysis were obtained from Matreya, LLC (Pleasant Gap, PA).

Lipid-bound and protein-bound sialic acid determination

Ganglioside isolation was performed as described under *Ganglioside isolation and TLC analyses*, except the initial precipitate containing all cellular proteins was allowed to dry at ambient temperature, then was fully solubilized in 0.1 M NaOH at ambient temperature. Aliquots of solubilized brain protein were neutralized with HCl, then dissolved in 0.1 M HCl, 0.25 M NaCl and heated at 80°C for 3 h. Aliquots of the acid hydrolysates were analyzed for sialic acid using Dionex strong anion exchange high performance liquid chromatography coupled with pulsed amperometric detection as described previously (Rohrer 2000). For direct comparison, aliquots of gangliosides purified from the same extract were evaporated to dryness, dissolved in 0.1 M HCl, 0.25 M NaCl and hydrolyzed as above. Aliquots of standard sialic acid of known concentration were hydrolyzed to correct for recovery.

Immunohistochemistry

IgG-class anti-ganglioside monoclonal antibodies GM1-1, GD1a-1, GD1b-1 and GT1b-1, developed by this laboratory and described previously (Schnaar et al. 2002), were used. Anti-MAG monoclonal antibody 513 was produced from hybridoma (Poltorak et al. 1987) kindly provided by Dr Melitta Schachner (Rutgers University, Piscataway, NJ). Adult mice (4–6 weeks old) were anesthetized with isoflurane and transcardially perfused with Dulbecco's phosphate-buffered saline (PBS) and then with 4% paraformaldehyde in PBS, pH 7.4. Brains were dissected, post-fixed overnight in the same fixative, then equilibrated and stored in 30% aqueous sucrose. Brains were frozen in isopentane at −80°C and 35–µm floating sections collected and stored in PBS at 4°C until staining. Sections were immunostained free-floating at 4°C in detergent-free buffers (Heffer-Lauc et al. 2007). Sections were treated with 0.2% hydrogen peroxide in PBS to reduce subsequent peroxidase background, then were blocked for 2.5 h in 5% (v/v) goat serum plus 1% (w/v) bovine serum albumin. Primary anti-ganglioside antibodies were added at 0.4–1.3 µg/mL and the sections incubated overnight, washed with PBS and then incubated for 4 h with 0.5 µg/mL biotin-

conjugated goat anti-mouse IgG (Jackson Immunoresearch, West Grove, PA). Sections were then washed with PBS, developed with Vector Elite horseradish peroxidase kit (Vector Laboratories, Burlingame, CA), stained with SigmaFast DAB with metal enhancer (Sigma-Aldrich, St Louis, MO), mounted on slides and air dried. MAG immunohistochemistry was performed using the same procedure with 1.2–1.5 μg/mL monoclonal antibody for primary incubations and 1% Triton X-100 in the blocking buffers.

Hindlimb reflex extension

Each mouse was lifted gently by the tail and held suspended for 10 s in three consecutive trials (Boyce et al. 1999). The position of the hindlimbs was scored as follows: 0, one or both hindlimbs paralyzed; 1, loss of reflex and hindlimbs and paws held close to the body with clasping toes; 2, loss of reflex with the flexion of hindlimbs; 3, hindlimbs extended to form <90° angle; 4, hindlimbs extended to form >90° angle.

Supplementary data

Supplementary data for this article is available online at http://glycob.oxfordjournals.org/.

Funding

This work was supported by NIH (NS037096 to R.L.S.) and was also supported by NIH (CA071932 and HL057345 to J. D.M.). The authors gratefully acknowledge access to the resources and expertise supported by NIH (P41 RR018502).

Conflict of interest

None declared.

Abbreviations

CID, collision-induced dissociation; LTQ, linear trap quadrupole. MAG, myelin-associated glycoprotein; MS, mass spectrometry; MS/MS, tandem mass spectrometry; PBS, phosphate-buffered saline; PCR, polymerase chain reaction; TLC, thin-layer chromatography. Ganglioside nomenclature is that of Svennerholm (1994).

References

Ando S. 1983. Gangliosides in the nervous system. *Neurochem Int*. 5:507–537.

Anumula KR, Taylor PB. 1992. A comprehensive procedure for preparation of partially methylated alditol acetates from glycoprotein carbohydrates. *Anal Biochem*. 203:101–108.

Aoki K, Perlman M, Lim JM, Cantu R, Wells L, Tiemeyer M. 2007. Dynamic developmental elaboration of N-linked glycan complexity in the *Drosophila melanogaster* embryo. *J Biol Chem*. 282:9127–9142.

Audry M, Jeanneau C, Imberty A, Harduin-Lepers A, Delannoy P, Breton C. 2011. Current trends in the structure–activity relationships of sialyltransferases. *Glycobiology*. 21:716–726.

Boyce S, Webb JK, Carlson E, Rupniak NM, Hill RG, Martin JE. 1999. Onset and progression of motor deficits in motor neuron degeneration (mnd) mice are unaltered by the glycine/NMDA receptor antagonist L-701,324 or the MAO-B inhibitor R(-)-deprenyl. *Exp Neurol*. 155:49–58.

Collins BE, Kiso M, Hasegawa A, Tropak MB, Roder JC, Crocker PR, Schnaar RL. 1997. Binding specificities of the sialoadhesin family of I-type lectins. Sialic acid linkage and substructure requirements for binding of myelin-associated glycoprotein, Schwann cell myelin protein, and sialoadhesin. *J Biol Chem*. 272:16889–16895.

Collins BE, Yang LJS, Mukhopadhyay G, Filbin MT, Kiso M, Hasegawa A, Schnaar RL. 1997. Sialic acid specificity of myelin-associated glycoprotein binding. *J Biol Chem*. 272:1248–1255.

Ellies LG, Ditto D, Levy GG, Wahrenbrock M, Ginsburg D, Varki A, Le DT, Marth JD. 2002. Sialyltransferase ST3Gal-IV operates as a dominant modifier of hemostasis by concealing asialoglycoprotein receptor ligands. *Proc Natl Acad Sci USA*. 99:10042–10047.

Ellies LG, Sperandio M, Underhill GH, Yousif J, Smith M, Priatel JJ, Kansas GS, Ley K, Marth JD. 2002. Sialyltransferase specificity in selectin ligand formation. *Blood*. 100:3618–3625.

Heffer-Lauc M, Viljetic B, Vajn K, Schnaar RL, Lauc G. 2007. Effects of detergents on the redistribution of gangliosides and GPI-anchored proteins in brain tissue sections. *J Histochem Cytochem*. 55:805–812.

Kawai H, Allende ML, Wada R, Kono M, Sango K, Deng C, Miyakawa T, Crawley JN, Werth N, Bierfreund U, et al. 2001. Mice expressing only monosialoganglioside GM3 exhibit lethal audiogenic seizures. *J Biol Chem*. 276:6885–6888.

Kojima N, Lee YC, Hamamoto T, Kurosawa N, Tsuji S. 1994. Kinetic properties and acceptor substrate preferences of two kinds of Gal beta 1,3GalNAc alpha 2,3-sialyltransferase from mouse brain. *Biochemistry*. 33:5772–5776.

Kolter T, Proia RL, Sandhoff K. 2002. Combinatorial ganglioside biosynthesis. *J Biol Chem*. 277:25859–25862.

Kono M, Ohyama Y, Lee YC, Hamamoto T, Kojima N, Tsuji S. 1997. Mouse β-galactoside α2,3-sialyltransferases: Comparison of in vitro substrate specificities and tissue specific expression. *Glycobiology*. 7:469–479.

Kono M, Takashima S, Liu H, Inoue M, Kojima N, Lee YC, Hamamoto T, Tsuji S. 1998. Molecular cloning and functional expression of a fifth-type alpha 2,3-sialyltransferase (mST3Gal V: GM3 synthase). *Biochem Biophys Res Commun*. 253:170–175.

Kracun I, Rosner H, Cosovic C, Stavljenic A. 1984. Topographical atlas of the gangliosides of the adult human brain. *J Neurochem*. 43:979–989.

Lee YC, Kurosawa N, Hamamoto T, Nakaoka T, Tsuji S. 1993. Molecular cloning and expression of Gal beta 1,3GalNAc alpha 2,3-sialyltransferase from mouse brain. *Eur J Biochem*. 216:377–385.

Liu Y, Wada R, Kawai H, Sango K, Deng C, Tai T, McDonald MP, Araujo K, Crawley JN, Bierfreund U, et al. 1999. A genetic model of substrate deprivation therapy for a glycosphingolipid storage disorder. *J Clin Invest*. 103:497–505.

Maccioni HJ, Quiroga R, Ferrari ML. 2011. Cellular and molecular biology of glycosphingolipid glycosylation. *J Neurochem*. 117:589–602.

Nimrichter L, Burdick MM, Aoki K, Laroy W, Fierro MA, Hudson SA, Von Seggern CE, Cotter RJ, Bochner BS, Tiemeyer M, et al. 2008. E-selectin receptors on human leukocytes. *Blood*. 112:3744–3752.

Okajima T, Fukumoto S, Miyazaki H, Ishida H, Kiso M, Furukawa K, Urano T, Furukawa K. 1999. Molecular cloning of a novel alpha2,3-sialyltransferase (ST3Gal VI) that sialylates type II lactosamine structures on glycoproteins and glycolipids. *J Biol Chem*. 274:11479–11486.

Pan B, Fromholt SE, Hess EJ, Crawford TO, Griffin JW, Sheikh KA, Schnaar RL. 2005. Myelin-associated glycoprotein and complementary axonal ligands, gangliosides, mediate axon stability in the CNS and PNS: Neuropathology and behavioral deficits in single- and double-null mice. *Exp Neurol*. 195:208–217.

Poltorak M, Sadoul R, Keilhauer G, Landa C, Fahrig T, Schachner M. 1987. Myelin-associated glycoprotein, a member of the L2/HNK-1 family of neural cell adhesion molecules, is involved in neuron-oligodendrocyte and oligodendrocyte-oligodendrocyte interaction. *J. Cell Biol.* 105:1893–1899.

Priatel JJ, Chui D, Hiraoka N, Simmons CJ, Richardson KB, Page DM, Fukuda M, Varki NM, Marth JD. 2000. The ST3Gal-I sialyltransferase controls CD8+ T lymphocyte homeostasis by modulating O-glycan biosynthesis. *Immunity*. 12:273–283.

Proia RL. 2003. Glycosphingolipid functions: Insights from engineered mouse models. *Philos Trans R Soc Lond B Biol Sci*. 358:879–883.

Rohrer JS. 2000. Analyzing sialic acids using high-performance anion-exchange chromatography with pulsed amperometric detection. *Anal Biochem*. 283:3–9.

Schauer R. 2009. Sialic acids as regulators of molecular and cellular interactions. *Curr Opin Struct Biol*. 19:507–514.

Schnaar RL. 1994. Isolation of glycosphingolipids. *Methods Enzymol*. 230: 348–370.

Schnaar RL. 2005. Brain glycolipids: Insights from genetic modifications of biosynthetic enzymes. In: Fukuda M, Rutishauser U, Schnaar RL, Yamaguchi Y, editors. *Neuroglycobiology*. Oxford (UK): Oxford University Press. p. 95–113.

Schnaar RL. 2007. Neural functions of glycolipids. In: Kamerling JP, Boons GJ, Lee YC, Suzuki A, Taniguchi N, Voragen AGJ, editors. *Comprehensive Glycoscience. Volume 4: Cell Glycobiology and Development; Health and Disease in Glycomedicine*. Amsterdam: Elsevier Science. p. 323–337.

Schnaar RL. 2010. Brain gangliosides in axon-myelin stability and axon regeneration. *FEBS Lett*. 584:1741–1747.

Schnaar RL, Fromholt SE, Gong Y, Vyas AA, Laroy W, Wayman DM, Heffer-Lauc M, Ito H, Ishida H, Kiso M, et al. 2002. Immunoglobulin G-class mouse monoclonal antibodies to major brain gangliosides. *Anal Biochem*. 302:276–284.

Schnaar RL, Lopez PH. 2009. Myelin-associated glycoprotein and its axonal receptors. *J Neurosci Res*. 87:3267–3276.

Schnaar RL, Needham LK. 1994. Thin-layer chromatography of glycosphingolipids. *Methods Enzymol*. 230:371–389.

Sonnino S, Ghidoni R, Chigorno V, Masserini M, Tettamanti G. 1983. Recognition by two-dimensional thin-layer chromatography and densitometric quantification of alkali-labile gangliosides from the brain of different animals. *Anal Biochem*. 128:104–114.

Sun J, Shaper NL, Itonori S, Heffer-Lauc M, Sheikh KA, Schnaar RL. 2004. Myelin-associated glycoprotein (Siglec-4) expression is progressively and selectively decreased in the brains of mice lacking complex gangliosides. *Glycobiology*. 14:851–857.

Svennerholm L. 1964. The gangliosides. *J Lipid Res*. 5:145–155.

Svennerholm L. 1994. Designation and schematic structure of gangliosides and allied glycosphingolipids. *Prog Brain Res*. 101:xi–xiv.

Svennerholm L, Bostrom K, Fredman P, Mansson JE, Rosengren B, Rynmark BM. 1989. Human brain gangliosides: Developmental changes from early fetal stage to advanced age. *Biochim Biophys Acta*. 1005:109–117.

Takamiya K, Yamamoto A, Furukawa K, Yamashiro S, Shin M, Okada M, Fukumoto S, Haraguchi M, Takeda N, Fujimura K, et al. 1996. Mice with disrupted GM2/GD2 synthase gene lack complex gangliosides but exhibit only subtle defects in their nervous system. *Proc Natl Acad Sci USA*. 93:10662–10667.

Tettamanti G, Bonali F, Marchesini S, Zambotti V. 1973. A new procedure for the extraction, purification and fractionation of brain gangliosides. *Biochim Biophys Acta*. 296:160–170.

Todeschini AR, Hakomori SI. 2008. Functional role of glycosphingolipids and gangliosides in control of cell adhesion, motility, and growth, through glycosynaptic microdomains. *Biochim Biophys Acta*. 1780:421–433.

Varki A. 1992. Diversity in the sialic acids. *Glycobiology*. 2:25–40.

Vukelic Z, Zamfir AD, Bindila L, Froesch M, Peter-Katalinic J, Usuki S, Yu RK. 2005. Screening and sequencing of complex sialylated and sulfated glycosphingolipid mixtures by negative ion electrospray Fourier transform ion cyclotron resonance mass spectrometry. *J Am Soc Mass Spectrom*. 16:571–580.

Yamashita T, Hashiramoto A, Haluzik M, Mizukami H, Beck S, Norton A, Kono M, Tsuji S, Daniotti JL, Werth N, et al. 2003. Enhanced insulin sensitivity in mice lacking ganglioside GM3. *Proc Natl Acad Sci USA*. 100:3445–3449.

Yang LJS, Zeller CB, Shaper NL, Kiso M, Hasegawa A, Shapiro RE, Schnaar RL. 1996. Gangliosides are neuronal ligands for myelin-associated glycoprotein. *Proc Natl Acad Sci USA*. 93:814–818.

Yu RK, Yanagisawa M, Ariga T. 2007. Glycosphingolipid Structures. In: Kamerling JP, Boons GJ, Lee YC, Suzuki A, Taniguchi N, Voragen AGJ, editors. *Comprehensive Glycoscience. Volume 1: Introduction to Glycoscience; Synthesis of Carbohydrates*. Amsterdam: Elsevier Science. p. 73–122.